JOURNAL OF CATALYSIS **179,** 56–63 (1998)
ARTICLE NO. CA982192

Interaction of Isobutene with the Surface of Different Solid Acids

Rajinder Gill, Lucía M. Petkovic, and Gustavo Larsen[1]

Department of Chemical Engineering, University of Nebraska, Lincoln Nebraska 68588-0126

Received February 10, 1998; revised June 15, 1998; accepted June 22, 1998

The interaction of an olefin with relatively high reactivity toward acid-catalyzed polymerization such as isobutene, with four different solid acids was investigated by means of *in situ* diffuse reflectance infrared spectroscopy (DRIFTS), continuous flow studies using a packed-bed oscillating balance reactor (OBR), and temperature-programmed desorption/reaction (TPD/R) of the preadsorbed olefin. The uptake of isobutene and its oligomers produced by acid-catalyzed surface polymerization at 473 K is very slow over H-ZSM-5, presumably due to a diffusion-controlled reaction process. The narrow pore structure of the zeolite prevents coke formation (cyclization), and the isobutene oligomers desorb slowly upon heating under nitrogen. In light of TPD/R and DRIFTS results, tungstated zirconia appears to be unable to undergo irreversible retention of isobutene and oligomeric products, whereas the two forms of sulfated zirconia investigated in this study retain a relatively large amount of oligomeric species, and subsequently produce coke and lose the sulfate function. There is a redox reaction between the surface carbonaceous residues and the sulfate function in sulfated zirconias. Of the four catalysts studied, sulfated zirconia systems were the most vulnerable to chemical attack by isobutene.

Key Words: **isobutene; DRIFTS; pulse mass analyzer; tungstated zirconia; H-ZSM-5; sulfated zirconia.**

INTRODUCTION

One of the mechanisms by which the skeletal rearrangement of alkanes occurs has been proposed to involve dimeric or oligomeric intermediates (1–5). The presence of C_{n+1} alkanes in the product mixture that results from reacting a C_n alkane over a strong solid acid catalyst is normally taken as evidence for such a mechanism. This is due to the fact that disproportionation of an alkane must involve more than just one reacting molecule, given the increased chain lengths observed in some of the product species (e.g., C_3 and C_5 produced from C_4). The presence of trace olefins is likely to be key to producing such oligomeric intermediates (5), especially for solid acids that do not reach superacidity levels and are therefore less likely to protonate the alkane. A natural (undesired) consequence of the bimolecular mechanism (Fig. 1) is that it almost certainly sets the stage for catalyst deactivation as well, since it could in principle turn into a conventional acid-catalized surface polymerization reaction. Aging of the resulting high-molecular species that are unable to desorb and free up the active sites leads to conventional coke, as they partially lose hydrogen, depending upon the temperature of the process.

Despite the fact that this deactivation mechanism has been known for many years, studies on the interaction of unsaturated hydrocarbons with zirconia-based solid acids are rare. Srinivasan *et al.* (6) have shown that benzene temperature-programmed desorption (TPD) cannot be used to study the acidity of sulfated zirconia (SZ) because this molecule adsorbs irreversibly on the surface of the catalyst and ultimately acts as a reducing agent, as evidenced by the evolution of CO_2 during TPD. On the other hand, we have studied the temperature-programmed desorption/reaction (TPD/R) of C_3 and C_4 alcohols over tungstated zirconia (WZ) and we noticed that this catalyst has a very low tendency to form olefin oligomers as secondary products (7,8). The opposite is true for H-Y and H-mordenite, i.e., m/e fragments corresponding to oligomeric olefins were detected in their TPD/R spectra (7,8). In addition, H^+/D^+ exchange between the acid sites and the alkyl chains was much more important in zeolites than in WZ. Since WZ and SZ are active catalysts for alkane isomerization, we speculated that the former may be a poor solid acid catalyst for effecting the surface polymerization of olefins. If this were true, the stability of this catalyst (9) could well be attributed to this phenomenon, whereas the low stability of SZ could be due to a combination of coking and loss of sulfate by a redox reaction. From a fundamental viewpoint, it appears interesting to compare the behavior of these catalysts in the presence of olefins with that of acidic zeolites. Thus, the main objective of this paper is to determine how olefins adsorb and react on the surface of WZ, SZ, and H-ZSM-5, how they interact with the active sites in each case, and how temperature affects such interactions.

While we are aware of the fact that the relationship between coke (or coke precursors) and catalytic activity is not always straightforward, we anticipate that our studies will be relevant to the issue of catalyst stability under conventional hydrocarbon feeds. For example, isobutene is known

---

[1] To whom all correspondence should be addressed.

0021-9517/98 $25.00

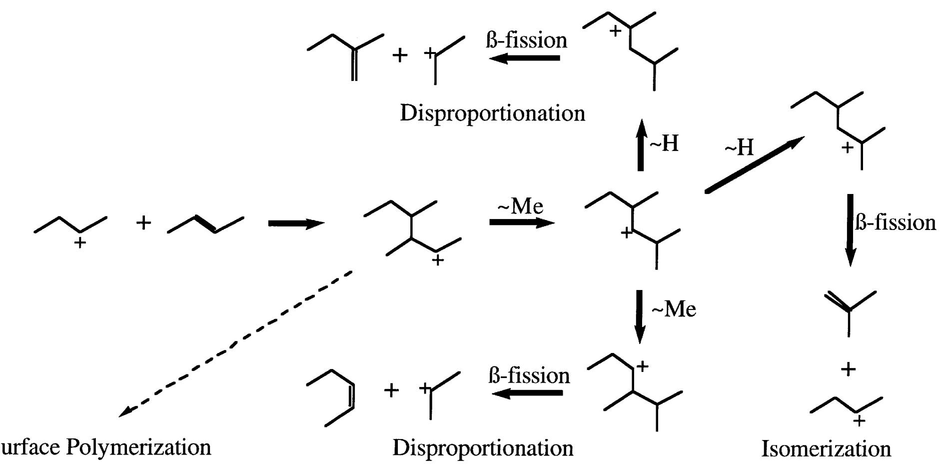

FIG. 1. Bimolecular mechanism of alkane isomerization (*n*-butane-to-isobutane case).

to be responsible, through oligomerization processes, for the deactivation of acidic zeolites during MTBE (10) and ETBE (11) synthesis. Sulfated zirconia is known to deactivate by either coke deposition or reduction of the sulfate function (12). A decrease in the oxidation state of sulfur has been proposed as the deactivation mechanism for SZ catalysts during *n*-butane (13), and 1-butene (14) isomerization. The presence of traces of isobutene in *n*-butane reacting over H-mordenite has been reported to increase the isomerization rate, in addition to the rate of side reactions such as coking and oligomerization (15). For other reactions involving alkenes, such as the alkylation of isobutane with butenes at low temperatures, SZ catalysts typically show high initial activities followed by fast deactivation (16).

EXPERIMENTAL

The preparation of tungstated zirconia catalysts has been described elsewhere (9). This catalyst was labeled as WZ and has a nominal 15 wt% WO_3 loading. Standard sulfated zirconia (4.3 wt% S) was prepared by soaking hydrous zirconia (obtained by precipitation with concentrated NH_3) in diluted H_2SO_4 (17). The Na-ZSM-5 is a sample from the International Committee on Catalyst Standards and has a 24.3 Si/2Al ratio. This sample was exchanged with a 1 *M* NH_4NO_3 solution (1-g catalyst/100-ml solution) for 24 h and subsequently calcined at 873 K for 1 h to obtain the H-ZSM-5 form. A 6.7 wt% S mesostructured form of sulfated zirconia (labeled as m-SZ) was prepared by a procedure described by our group recently (18). In brief, the method makes use of dodecyl sulfate as a template at 363 K, followed by a $SO_4^=$ loading/surfactant washing step with $(NH_4)_2SO_4$. This catalyst belongs to the class of disordered mesoporous structures (19,20) in which pore diameter, rather than pore ordering, is conserved. Our method also results in surface areas which are about twice as large as those found in conventional SZ catalysts, i.e., 215 m^2/g (11) versus 90–110 m^2/g (21). The m-SZ catalyst has shown to be very active for *n*-butane isomerization (18). The WZ sample has a BET surface area of 25 m^2/g. Ultra-high purity gases from Linweld, Lincoln, were further purified with commercial oxygen traps from Supelco®. Research grade isobutene from Linweld (99.75% purity) was used without further purification.

A conventional atmospheric, gas-phase stainless-steel flow reaction system equipped with Brooks 5850 mass-flow controllers was used for the temperature-programmed desorption/reaction runs. An MKS® Residual Gas Analyzer was used to follow up to 16 different m/e signals. The catalyst bed (typically 250 mg) was placed in a 8-mm ID quartz U-tube, preceded by a preheating bed composed of α-Al_2O_3 (1–2 m^2/g) particles. The samples were pelletized, followed by crushing and sieving, to collect the 20–45 mesh fraction. The temperature was controlled externally to ±0.5 K. All samples were pretreated *in situ* prior to the TPD/R experiments. Five successive 1-ml isobutene pulses were allowed upstream of the U-tube reactor at 473 K with the catalyst under flowing N_2 (100 cc/ min.). The catalysts were purged under the same N_2 flow for another 20 min to remove reversibly adsorbed species, and the temperature was ramped at a 7.2 K/min rate up to 1073 K. We carefully selected a large number of m/e ratios indicative of olefin oligomerization (e.g., 65, 55, 69, etc.), active phase loss (SO_2^+, SO^+, WO^+ fragments) and redox processes (CO_2^+, CO^+, etc.). In the TPD/R figures below, we show only the detectable m/e ratios.

In situ DRIFTS studies were carried out on a Nicolet 20 SXB Fourier transform infrared spectrometer equipped with a commercial DRIFTS catalytic chamber and associated optical and temperature control systems from Spectratech®. The reactor part of the cell consists of a temperature-controlled ceramic cup, where the catalyst powder is packed and reactants are allowed to flow through. A similar stainless steel mass-flow controlled reaction system to that described in the previous paragraph was used. Typically, 0.05 g of a powdered catalyst sample were placed in the DRIFTS cell and pretreated *in situ* prior to the DRIFTS runs. Once the temperature was stabilized at 473 K, a pure isobutene flow was allowed in the cell for 15 min, followed by a purging period of 20 min under 40 cc/min N_2. Data were collected for approximately 18 min in the 4000–400 cm^{-1} wavenumber interval, at 4 cm^{-1} optical resolution. Keeping the sample under flowing N_2, the temperature was raised in 100 K intervals and spectra were collected again at each temperature. Spectra are presented after the Fourier-transformed data in a reflectance scale has been converted to Kubelka–Munk units.

The concept of the oscillating balance reactor (OBR) was initially developed for the quantification of particulates in air (22) and was not adapted for *in situ* catalysis research until recent times (23–25). The basic idea is that the catalyst cell is made to oscillate at its natural frequency, and an instantaneous weight change in the packed bed can easily be monitored because it translates into a frequency change that is detected and processed by a computer. It has the ability to detect minute weight changes with excellent mass-time resolution, and the flow profile is much better defined than the flow regimes that take place in conventional microbalances, due to its packed-bed geometry (Fig. 2). A commercial unit from the R&P® company was used in our studies. The oscillating element allows for the pretreatment of samples *in situ*. The WZ sample required calcination at 1096 K (9) and for that reason, this sample was calcined *ex situ* and reactivated in the OBR cell, since the latter only allows heating up to 873 K. The OBR apparatus is also interfaced with a stainless steel, mass-flow controlled reaction manifold essentially identical to those of the DRIFTS and the TPD/R units. Upon pretreatment of the samples (50 mg), the temperature was stabilized under a nitrogen flow of 48 cc/min for 15 min to produce a stable signal. The OBR cell was then bypassed and an isobutene flow of 20 cc/min was set. The experiments were run at atmospheric pressure. Recording of data begun immediately after the isobutene flow was switched from the bypass to the cell line. An inert packed bed of α-Al_2O_3 (1–2 m^2/g) was used for a blank run, since the switching of gases with different densities (from N_2 to isobutene) causes a mass change that is not due to adsorption phenomena and needs to be subtracted from the actual runs (23).

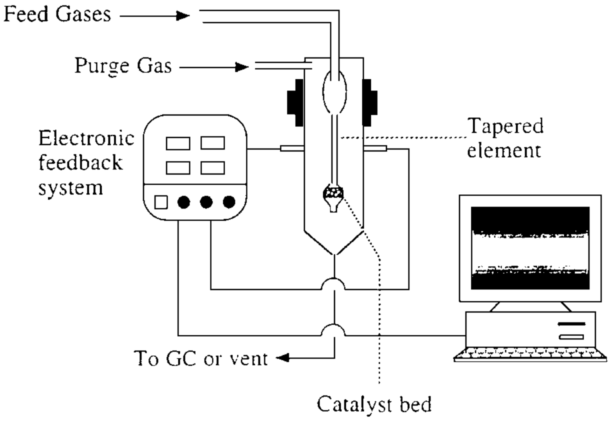

FIG. 2. Oscillating balance reactor setup.

RESULTS AND DISCUSSION

Figures 3A–B show the retention of isobutene and/or isobutene oligomers under continuous isobutene flow using the OBR apparatus. We have chosen to report our results on a mass basis because the acid sites present in these three catalysts differ markedly in nature from sample to sample.

A slow retention of isobutene by the purely protic solid acid (H-ZSM-5) is immediately apparent, presumably due to a diffusion-limited oligomerization process (26). Trombetta *et al.* (26) have stressed the fact that a diffusion-limited polymerization takes place when isobutene is allowed to react over H-ZSM-5, but the situation is different with linear butenes because such olefins are less affected by steric effects. On the other hand, the retention of isobutene and its oligomers over less stable solid acids such as SZ and *m*-SZ is much more significant. During the first 0.5–1 h reaction, the WZ sample appears to adsorb isobutene at comparable levels to those of the zeolite, but the rates of isobutene adsorption/oligomerization of these two samples was very different. The isobutene/S ratios at the plateau uptakes in m-SZ and SZ are a clear indication that not all the surface sulfate was active in these two materials. We found these ratios to be 0.12 and 0.20 for m-SZ and SZ, respectively. Similarly, an isobutene/W ratio equal to 0.21 was calculated for the WZ sample, but it should be emphasized that the active site in this material may involves more than one tungsten center.

Another interesting observation is the fast retention of olefinic species in the zirconia-based solid acids with respect to that of the zeolite. Diffusion of isobutene is expected to be faster in the former. In all three cases, a plateau was reached. This must be due to either adsorption saturation, pore plugging, or loss of active phase by chemical attack. We will later discuss the different possibilities in light of TPD/R and DRIFTS results. We have no simple explanation for the modest maximum in olefin retention as a function of time on stream observed in SZ. One possibility is that the carbonaceous material in the surface lose some hydrogen with time on stream.

The key question at this point is, how do we distinguish between isobutene and its oligomers?. We then carried out the DRIFTS experiments to follow the chemical evolution

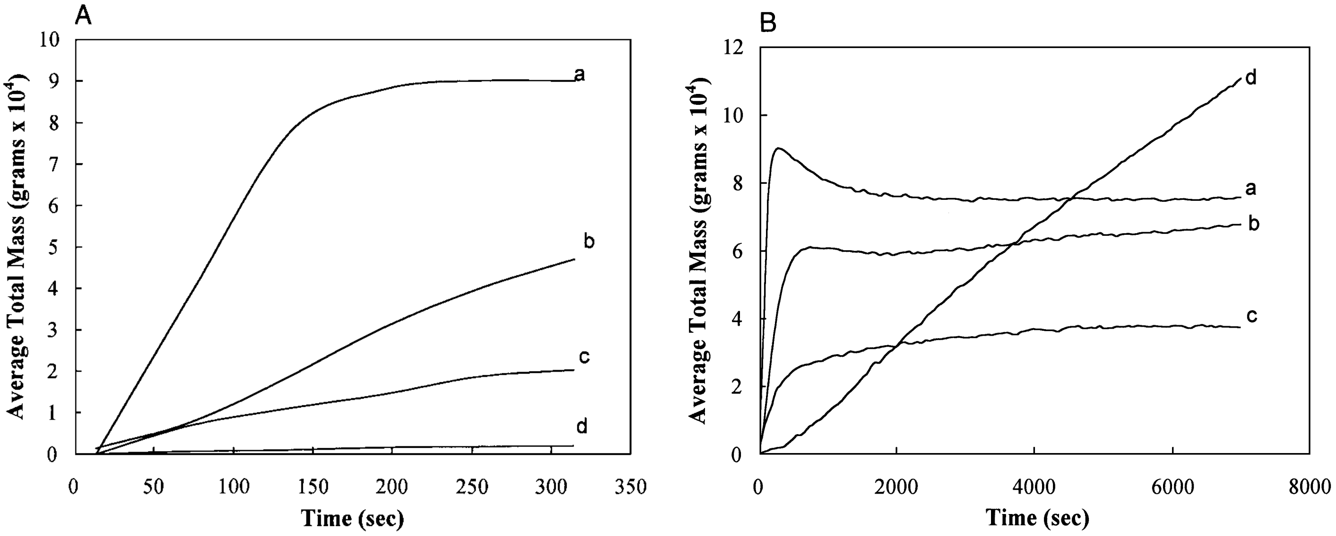

FIG. 3. Retention of isobutene and/or isobutene oligomers under continuous isobutene flow: (a) SZ; (b) m-SZ; (c) WZ; (d) H-ZSM-5. Conditions: continuous isobutene flow at 473 K, $P = 1$ atm. Isobutene: 60 g (g cat.)$^{-1}$ h^{-1}. (A) At short times on stream; (B) at long times on stream.

of the adsorbed species upon purging and heating. Figures 4A–B show that nearly no hydrocarbons remain at the WZ surface upon isothermal purging (see the extremely weak C-H stretching signal around 2950 cm^{-1} in Fig. 4A), and no coke bands are evident upon heating under nitrogen (Fig. 4B). Since WZ has also shown to be a very poor oligomerization catalyst for olefin primary products resulting from alcohol dehydration reactions (7,8), we are led to infer that olefins adsorb reversibly on WZ. On the other hand, Fig. 5A shows that hydrocarbon species, expected to be oligomeric isobutene (26), do not desorb from the H-ZSM-5 catalyst at 473 K upon N$_2$ purging, but they do so slowly upon heating. Note the shift in the low-frequency OH stretching (the acidic OH group in zeolites) toward lower frequencies when isobutene is allowed in the DRIFTS cell. Spoto *et al.* (27) studied the polymerization of ethylene and propylene over H-ZSM-5 and concluded that this frequency shift is due to the perturbation of the OH group by the oligomeric alkyl chains. The acidic OH stretching signal of the free zeolite is restored upon thermal desorption of the oligomers.

The assignment of infrared bands for the CH stretching modes is, $\nu_{\mathrm{as\,CH2}}$ (aliphatic) ~ 2930–2940 cm^{-1}, $\nu_{\mathrm{s\,CH2}}$ (aliphatic) ~ 2860 cm^{-1}, $\nu_{\mathrm{as\,CH2}}$ (olefinic) ~ 3080 cm^{-1}, $\nu_{\mathrm{as\,CH3}}$ (aliphatic) ~ 2960–2970 cm^{-1}, and $\nu_{\mathrm{C=C}}$ ~ 1640–1650 cm^{-1} (28). All three assignments for the aliphatic signals

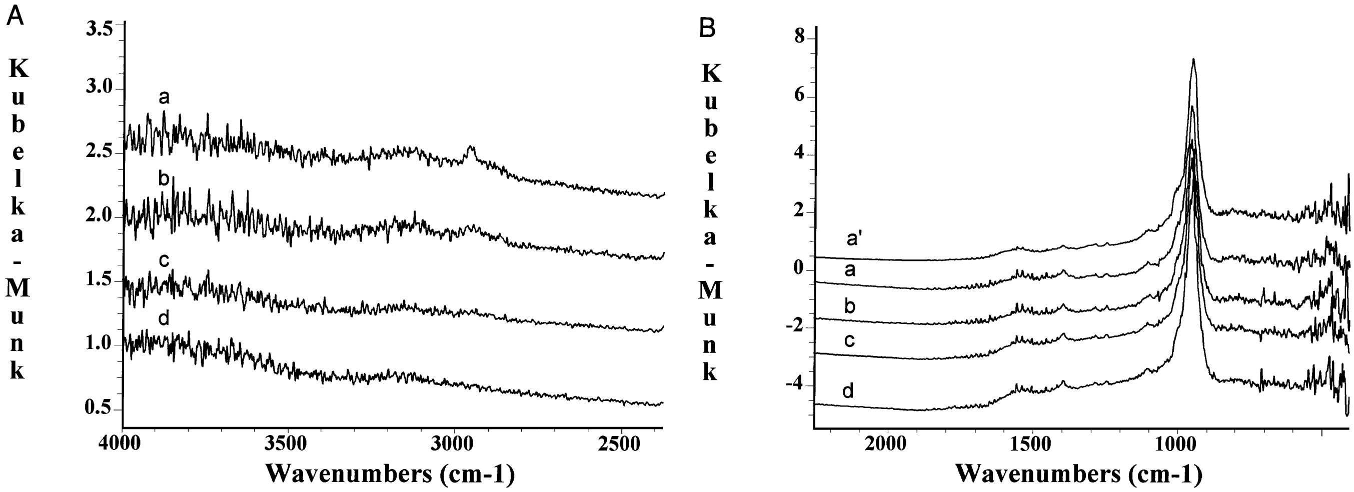

FIG. 4. DRIFTS spectra of irreversibly adsorbed isobutene at 473 K over WZ: (A) Difference spectra in the C-H stretching region. Spectra upon heating at (a) 473 K, (b) 573 K, (c) 673 K, and (d) 773 K, subtracted from those of the catalyst at the same temperature. (B) Spectra in the C=C and C-C stretching and C-H deformation region. Upon heating at (a) 473 K, (b) 573 K, (c) 673 K, and (d) 773 K; (a′) spectrum at 473 K prior to adsorption.

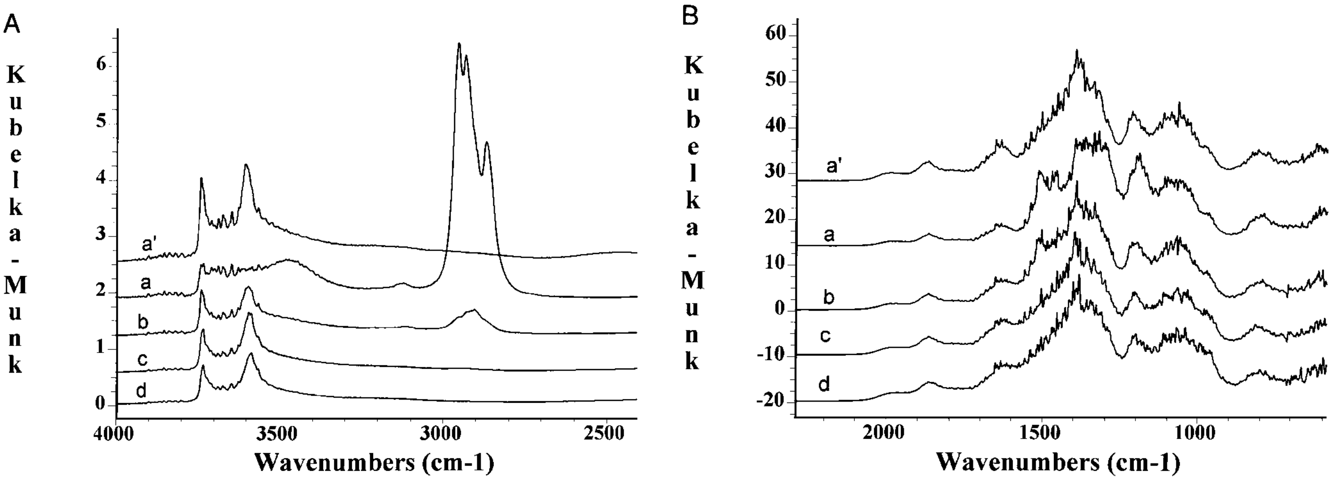

FIG. 5. DRIFTS spectra of irreversibly adsorbed isobutene at 473 K over H-ZSM-5: (A) spectra in the C-H stretching region; (B) spectra in the C=C and C-C stretching and C-H deformation region. Upon heating at (a) 473 K, (b) 573 K, (c) 673 K, and (d) 773 K; (a′) spectrum at 473 K prior to adsorption.

agree well with the three peaks observed in Fig. 5A. In addition, note that a very small signal around 3100 cm^{-1} is apparent in that figure. This signal is assigned to free, terminal double bonds, $\nu_{\mathrm{as\,CH2}}$ (olefinic). Since the relative intensity of the $\nu_{\mathrm{as\,CH2}}$ (olefinic) signal is much larger in isobutene (28), we take this observation as indicative of either formation of carbenium-like species, or oligomerization, because the CH signals from saturated CH groups largely dominate the DRIFTS spectrum in that region. In Fig. 5B, it is apparent that no coke is formed upon heating, given the absence of coke bands in the 1590 cm^{-1} region (29–30). Bands around 1300–1450 cm^{-1} may be assigned to saturated CH deformations. The SZ catalyst retains isobutene and oligomeric isobutene; then these species lose hydrogen upon heating (see the gradual disappearance of the C-H stretching bands and the appearance of a broad $\nu_{\mathrm{as\,CH2}}$ (olefinic) signal in Fig. 6A). This process causes the double penalty of destroying the sulfate function by reduction (see the disappearance of the 1380 cm^{-1} S=O band in Fig. 6B), and coke generation (shoulders at ca 1600 cm^{-1} in Fig. 6B). Sachtler *et al.* (31) have detected a marked decrease in the 1380 cm^{-1} sulfate band upon reduction of SZ with hydrogen. These authors concluded that a sulfide form remained at the surface after reduction. While there is a fair probability for this phenomenon to occur, such $S^{=}$ species must be in a form that is not detectable by DRIFTS because we found none for the presence of surface-SH groups. Interestingly, we also found no evolution of SO_x species or SH_2

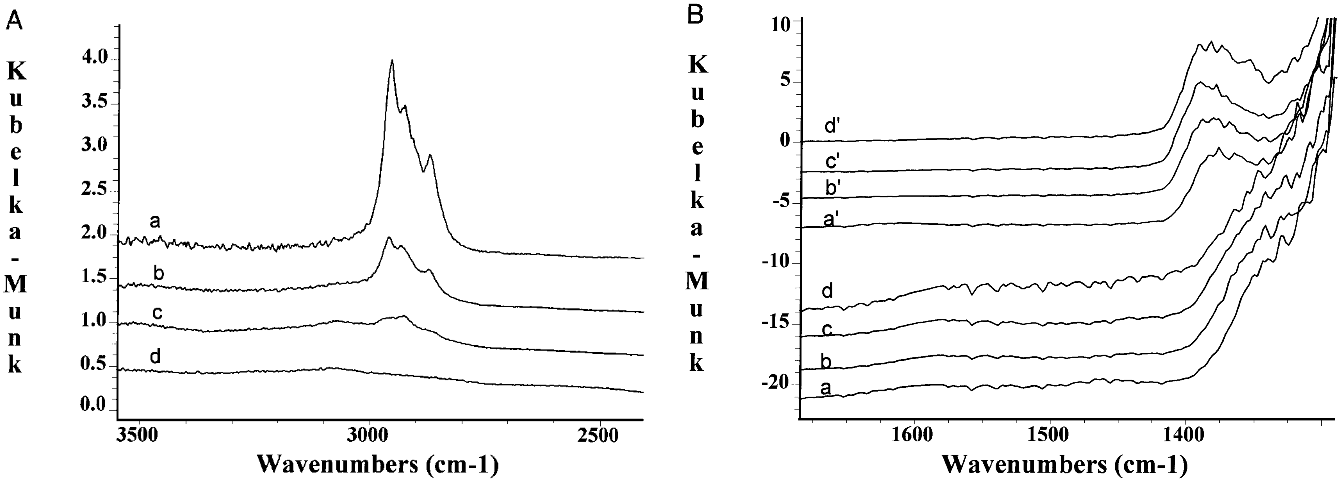

FIG. 6. DRIFTS spectra of irreversibly adsorbed isobutene at 473 K over SZ: (A) Difference spectra in the C-H stretching region. Spectra upon heating at (a) 473 K, (b) 573 K, (c) 673 K, and (d) 773 K, subtracted from those of the catalyst at the same temperature. (B) Spectra in the C=C and C-C stretching and C-H deformation region upon heating at (a) 473 K, (b) 573 K, (c) 673 K, and (d) 773 K. Blanks are (a′) 473 K, (b′) 573 K, (c′) 673 K, and (d′) 773 K.

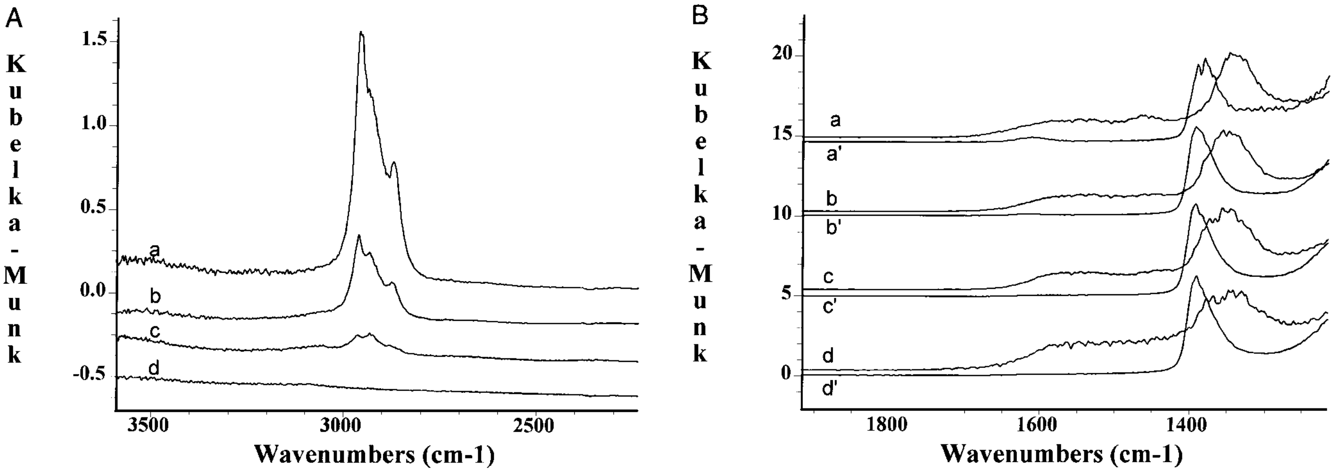

FIG. 7. DRIFTS spectra of irreversibly adsorbed isobutene at 473 K over m-SZ: (A) Difference spectra in the C-H stretching region. Spectra upon heating at (a) 473 K, (b) 573 K, (c) 673 K, and (d) 773 K, subtracted from those of the catalyst at the same temperature. (B) Spectra from the C=C and C-C stretching and C-H deformation region. Upon heating at (a) 473 K, (b) 573 K, (c) 673 K, and (d) 773 K. Blanks are (a′) 473 K, (b′) 573 K, (c′) 673 K, and (d′) 773 K.

at 473 K during the isothermal injection of the isobutene pulses prior to the TPD/R experiments.

The m-SZ on the other hand, displays a similar behavior to that of SZ in the CH stretching region. Bands at 2800–3000 cm^{-1} (Fig. 7A) are consistent with saturated species, whereas the lack of a signal around 3100 cm^{-1} associated with olefinic species is an indication that oligomerization (and/or formation of carbenium-like species) on m-SZ has occurred to a larger extent than that on H-ZSM-5, in which a small but detectable vinyl C-H stretching signal around 3100 cm^{-1} was found.

At this point, it must be mentioned that sharper S=O stretching features are often observed in the transmission IR spectra of sulfated zirconia catalysts, but it must be understood that DRIFTS bandwidths and intensities are strongly affected by crystallite size and by the pressure applied when loading a powdered sample (32,33). Given the textural differences between m-SZ and SZ, it would then be more appropriate to compare the effect of temperature and change in gas environment on the DRIFTS spectrum of a catalyst, rather than between catalysts. Still, isobutene has a different effect on the sulfate function of m-SZ relative to SZ (see Fig. 7B). The S=O stretching does not disappear as in the m-SZ case. Instead, it shifts to lower frequencies to a value (ca 1320 cm^{-1}) that is consistent with adsorbed sulfite species (34), rather than with $SO_{3\,ads}$ or $H_2SO_{4\,ads}$ forms (35). Furthermore, both SZ and m-SZ spectra before isobutene contact presented a small ν_{OH} band at around 3640 cm^{-1} that disappeared upon olefin exposure. Band shifts for the OH group after different base adsorption on sulfated zirconia has been reported to correlate with Bronsted acid strength (36). The higher resistance of the m-SZ toward sulfur reduction is a condition that is not expected to be due to mere pore size differences. It must be due to differences in catalyst preparation procedure. For example, to synthesize m-SZ, $(NH_4)_2SO_4$ is used as the sulfate source, which is in turn loaded at 363 K in an aqueous-organic medium (18). While we noticed no obvious differences between the IR spectra of these two catalysts in the sulfate region prior to isobutene adsorption, there must be a different sulfate binding mechanism operating in each case.

When TPD/R of isobutene adsorbed at 473 K was carried out under flowing N_2, no oligomers were found to desorb from SZ, but the sulfate function was lost as SO_2 at around 950 K (Fig. 8). Since we detected no oxygen evolution, we conclude that the SO_2 is formed by the reaction of sulfur species with the support and/or coke. In addition,

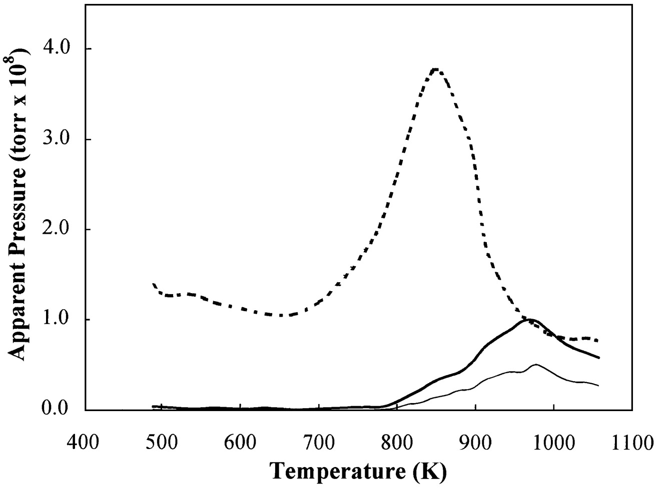

FIG. 8. TPD/R of irreversibly adsorbed isobutene at 473 K over SZ: *m/e*: (━━) 64, (——) 48, (············) 44; *m/e* followed: 41, 55, 65, 69, 18, 44, 28, 14, 113, 71, 80, 64, 48, 34, 33, 32.

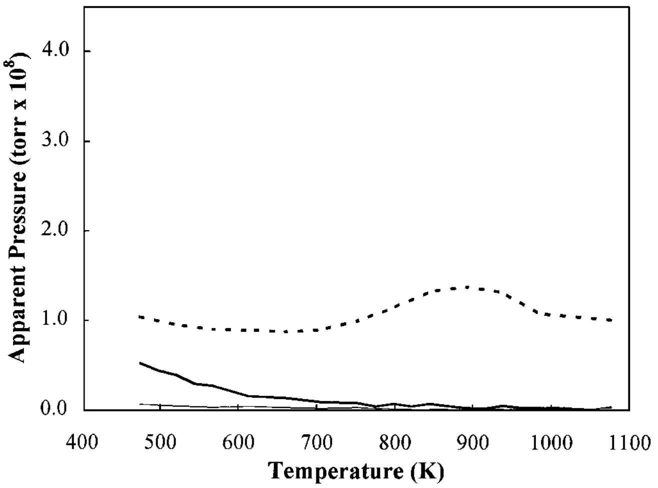

FIG. 9. TPD/R of irreversibly adsorbed isobutene at 473 K over m-SZ: *m/e*: (——) 41, (——) 71, (············) 44; *m/e* followed: 41, 55, 65, 69, 18, 44, 28, 14, 113, 71, 80, 64, 48, 34, 33, 32.

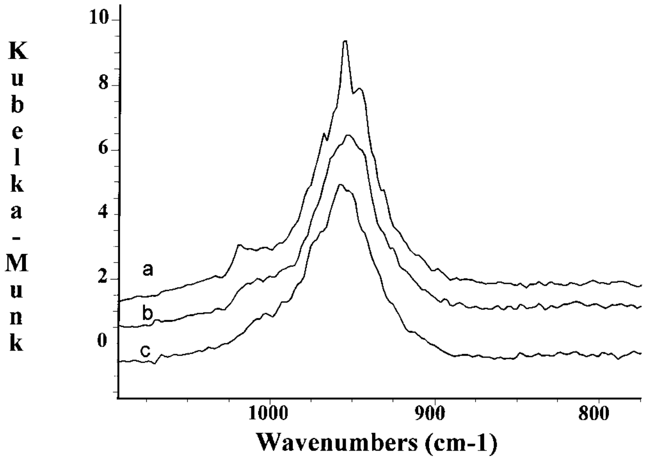

FIG. 11. DRIFTS spectra in the W=O region at 623 K: (a) before reduction; (b) after reduction; and (c) after isobutylene pulses. This WZ sample is 12 wt% WO_3.

CO_2 was formed during the TPD/R, which is consistent with the observations made by Srinivasan *et al.* (6) with regard to benzene TPD over SZ. Interestingly, the higher stability of sulfur-containing species in the m-SZ catalyst with respect to conventionally prepared SZ was also confirmed by this technique (Fig. 9), as evidenced by the absence of SO_2 signals. It appears that there is a strong redox interaction between the active phase and the carbonaceous residues. It has been proposed that the high isomerization activity of SZ could be attributed to an unusual one-electron oxidizing ability of the active site (37). The SO_x-esters formed upon alkane adsorption could then ionize and yield surface carbocations (37). In light of our results on the interaction of isobutene with the two forms of SZ catalysts investigated here, we are inclined to believe that irreversible damage of the active function of SZ occurs by a redox process in the presence of gas phase olefins. While it can be argued that the *n*-butane isomerization reaction is normally run under a large excess of alkane and perhaps only trace amounts of olefins, it is difficult to believe that *n*-butane (which is chemically more reduced than olefins) could revert the type of redox poisoning described here.

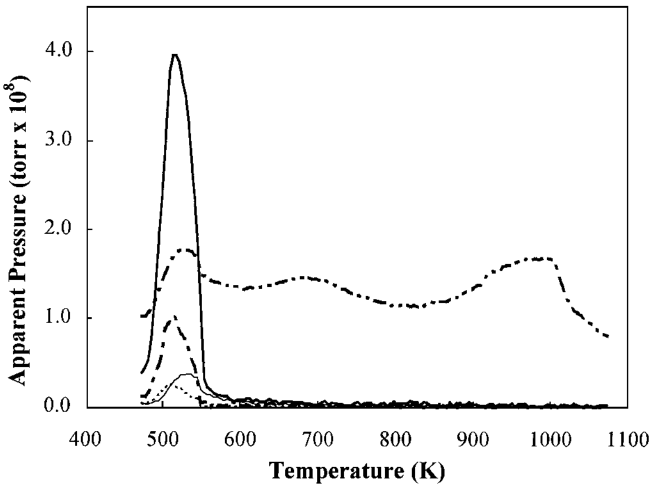

FIG. 10. TPD/R of irreversibly adsorbed isobutene at 473 K over H-ZSM-5: *m/e*: (——) 41, (–·–·–·–) 55, (············) 71, (——) 65, (–··–··–··–) 44; *m/e* followed: 41, 55, 65, 69, 18, 44, 28, 14, 113, 71, 80, 64, 48, 34, 33, 32.

In Fig. 10, it is shown that the H-ZSM-5 catalyst showed desorption of oligomers (m/e 55, 69, etc.) at about 530 K. We have at this point no easy answer to the small but detectable CO_2 signal found in the TPD in Fig. 10. One possibility is that this was due to a reaction between a trace, IR-undetectable amount of coke and some reducible impurity in the zeolite. On the other hand, we do not present the TPD results on the WZ catalyst because this sample showed no evolution of CO_2, oligomers, or loss of active phase (WO^+ fragments) upon heating up to 1100 K under N_2. Irreversible changes in this catalyst were not detected by DRIFTS and TPD/R. It must be stressed that the tungsten function under typical alkane isomerization reaction conditions is expected to be in a partially reduced state (38,39). The intense blue coloration of WZ upon hydrogen reduction and/or reaction is reminiscent of the chemistry of tungsten bronzes (40,41) and tungsten oxide-based electrochromic devices (42). By means of *in situ* DRIFTS, we have noticed that a band around 1019 cm^{-1}, which is associated with catalyst activity (43), becomes broader and shifts to lower frequencies upon reduction of WZ at 623 K (44). This band is also affected (Fig. 11) by the presence of olefins.

CONCLUSION

Our results show important changes in the surface of SZ catalysts to occur in the presence of olefins. It is conceivable that such changes have been generally overlooked in the past because much lower olefin concentrations were present in the majority of the alkane isomerization catalytic tests reported so far. Furthermore, such changes cannot occur in this acidic zeolite because of pore constraints. Kogelbauer *et al.* (10) described three possible ways by which isobutene can react over acidic zeolites. These are: (i) a proton transfer mechanism producing a protonated isobutene carbocation, (ii) a covalently bonded alkyl silyl ether, or (iii) a hydrogen-bonded isobutene intermediate. Note that none of these involve redox chemistry. However, the absence of redox phenomena on zeolites cannot be entirely ruled out. Electron acceptor and donor properties have been attributed to zeolites (45). For example, 1-pentene and benzene appear to undergo oxidation over Y-zeolites exchanged with either H^+, Ca^{++}, or rare-earth cations (45). Metal impurities, Brønsted, or Lewis sites, and especially positive (oxygen atom) holes created by oxidative processes upon high-temperature treatments have been proposed to play a role in the electron accepting properties of zeolites (46). Such intriguing redox chemistry in zeolites will benefit from future studies. At this point, we favor the interpretation of Kogelbauer *et al.* (10) concerning the interaction of isobutene with protic zeolites.

Unlike sulfated zirconia catalysts, olefins are expected to adsorb reversibly over WZ around 473 K. This feature may play a critical role in the stability of this catalyst for acid-catalyzed reactions in which alkenes are supposed to generate reactive intermediates. An important point to be made is that the stability of H-ZSM5 toward coking is due to physical phenomena (e.g., pore size constraints), rather than to an intrinsic chemical resistance, as in the WZ case.

ACKNOWLEDGMENTS

We thank an Engineering Research Equipment Grant from the NSF (CTS-9610315) that allowed us to purchase the vibrational microbalance reactor, and the Donors of the Petroleum Research Fund (31067-AC5). Funds from the Nebraska Research Initiative were used to support RG's graduate work, while LMP thanks the U. of San Juan (Argentina) for supporting her graduate work at the University of Nebraska. We are also indebted to Dr. Daniel Resasco for the chemical analysis of the SZ samples and to Edgar Lotero for the preparation of the m-SZ sample.

REFERENCES

1. Brower, D. M., *in* "Chemistry and Chemical Engineering of Catalytic Processes" (R. Prins and G. C. A. Schuit, Eds.). Sijthoff Noordhoff, Amsterdam, 1980.
2. Adeeva, V., Lei, G. D., and Sachtler, W. M. H., *Appl. Catal. A: Gral.* **118**, L11 (1994).
3. Larsen, G., and Petkovic, L. M., *J. Mol. Catal.* **113**, 517 (1996).
4. Rezgui, S., and Gates, B. C., *Catal. Lett.* **37**, 5 (1996).
5. Tábora, J. E., and Davis, R. J., *J. Amer. Chem. Soc.* **118**, 12240 (1996).
6. Srinivasan, R., Keogh, R. A., Ghenciu, A., Farcasiu, D., and Davis, B. H., *J. Catal.* **158**, 502 (1996). [References cited therein]
7. Larsen, G., Lotero, E., Nabity, M., Petkovic, L. M., and Querini, C. A., *Stud. Surface Sci. Catal.* **111**, 147 (1997).
8. Larsen, G., Lotero, E., Petkovic, L. M., and Shobe, D. S., *J. Catal.* **169**, 67 (1997).
9. Larsen, G., Lotero, E., Raghavan, S., Parra, R. D., and Querini, C. A., *Appl. Catal. A: Gral.* **139**, 201 (1996).
10. Kogelbauer, A., Nikolopoulos, A. A., Goodwin, J. G. (Jr.), and Marcelin, G., *J. Catal.* **152**, 122 (1995).
11. Larsen, G., Lotero, E., Marquez, M., and Silva, H., *J. Catal.* **157**, 645 (1995).
12. Song, X., and Sayari, A., *Catal. Rev. Sci. Eng.* **38**(3), 329 (1996).
13. Yori, J. C., Luy, J. C., and Parera, J. M., *Appl. Catal.* **46**, 103 (1989).
14. Sohn, J. R., and Kim, H. W., *J. Molec. Catal.* **52**, 361 (1989).
15. Fogash, K. B., Hong, Z., and Dumesic, J. A., *J. Catal.* **173**, 519 (1998).
16. Corma, A., Martínez, A., and Martínez, C., *J. Catal.* **149**, 52 (1994).
17. Iglesia, E., Soled, S. L., and Kramer, G. M., *J. Catal.* **144**, 238 (1993).
18. Larsen, G., Lotero, E., Nabity, M., Petkovic, L. M., and Shobe, D. S., *J. Catal.* **164**, 246 (1996).
19. Ryoo, R., Kim, J. M., and Shin, C. H., *J. Phys. Chem.* **100**, 17718 (1996).
20. Lei, G. D., Carvill, B. T., and Sachtler, W. M. H., *Appl. Catal. A: Gral.* **142**, 347 (1996).
21. Larsen, G., Lotero, E., Parra, R. D., Petkovic, L. M., Silva, H. S., and Raghavan, S., *Appl. Catal. A: Gral.* **130**, 213 (1995).
22. Patashnick, H., Rupprecht, G., and Wang, J. C. F., *Prepr.-Am. Chem. Soc., Div. Petr. Chem.* **25**, 188 (1980).
23. Fung, S. C., Querini, C. A., Liu, K., Rumschitzki, D. S., and Ho, T. C., *Stud. Surf. Sci. Catal.* **88**, 305 (1994).
24. Liu, K., Fung, S. C., and Rumschitzki, D. S., *J. Catal.* **169**, 455 (1997).
25. Hershkowitz, F., and Madiara, P. D., *Ind. Eng. Chem. Res.* **32**, 2969 (1993).
26. Trombetta, M., Busca, G., Rossini, S., Piccoli, V., and Cornaro, U., *J. Catal.* **168**, 349 (1997).
27. Spoto, G., Bordiga, S., Ricchiardi, G., Scarano, D., Zecchina, A., and Borello, E., *J. Chem. Soc. Far. Trans.* **90**, 2827 (1994).
28. Nyquist, R. A., "The Interpretation of Vapor Phase Infrared Spectra," Sadtler Research Laboratories, PA, 1984.
29. Blackmond, D. G., Goodwin Jr., J. G., and Lester, J. E., *J. Catal.* **78**, 34 (1982).
30. Karge, H. G., Nießen, W., Bludau, H., *Appl. Catal. A: Gral.* **146**, 339 (1996).
31. Xu, B.-Q., Sachtler, W. M. H., *J. Catal.* **167**, 224 (1997).
32. Griffiths, P. R., Fuller, M. P., *in* "Advances in Infrared and Raman Spectroscopy" (R. J. H. Clark and R. E. Hester, Eds.), Vol. 9. Heyden, London, 1986.
33. Hamadeh, I. M., King, D., and Griffiths, P. R., *J. Catal.* **88**, 264 (1984).
34. Waqif, M., Saad, A. M., Bensitel, M., Bachelier, J., Saur, O., and Lavalley, J.-C., *J. Chem. Soc. Faraday Trans.* **88**(19), 2931 (1992).
35. Babou, F., Coudurier, G., and Vedrine, J. C., *J. Catal.* **152**, 341 (1995).
36. Song. X., and Sayari, A., *Catal. Rev.-Sci. Eng.* **38**(3), 329 (1996).
37. Farcasiu, D., Ghenciu, A., and Li, J. Q., *J. Catal.* **158**, 116 (1996).
38. Santiesteban, J. G., Vartuli, J. C., and Chang, C. D., *J. Catal.* **168**, 431 (1997).
39. Larsen, G., Lotero, E., and Parra, R. D., *in* "11th International Congress on Catalysis-40th Anniversary, Stud. in Surf. Sci. and Catal." (J. W. Hightower *et al.*, Eds.), Vol. 101, p. 543. Elsevier Science, Amsterdam, 1996.
40. Khoobiar, S., *J. Phys. Chem.* **68**, 411 (1964).
41. Benson, J. E., Kohn, H. W., and Boudart, M. J., *J. Catal.* **5**, 307 (1966).
42. Paul, J.-L., and Lassegues, J. C., *J. Sol. State Chem.* **106**, 357 (1993).
43. Boyse, R. A., and Ko, E. I., *J. Catal.* **171**, 191 (1997).
44. Petkovic, L. M., Bielenberg, J. R., and Larsen, G., *J. Catal.*, in press.
45. Yoon, K. B., *Chem. Rev.* **93**, 321 (1993).
46. Shih, S., *J. Catal.* **79**, 390 (1983).